

# MBM 12 and MBM 16 distances

J. Knude<sup>1\*</sup> and H. E. P. Lindstrøm<sup>1,2\*</sup>

<sup>1</sup>*Niels Bohr Institutet, Copenhagen University, Juliane Maries Vej 30, DK-2100 København Ø, Denmark*

<sup>2</sup>*CSC Danmark A/S, Retortvej 8, DK-2500 Valby, Denmark*

Accepted 2012 Month 99. Received 2012 Month 99; in original form 2012 Month 99

## ABSTRACT

Among the multitude of intrinsic SDSS index vs. index diagrams the  $(g-r)$  vs.  $(r-i)$  diagram is characterized by showing only minor  $(g-r)$  variation for the M dwarfs. The  $(g-r)$  vs.  $(r-i)$  reddening vector has a slope almost identical to the slope of the main sequence earlier than  $\approx M2$ , meaning that dwarfs later than  $\sim M2$  are not contaminated by reddened dwarfs of earlier type. Chemical composition, stellar activity and evolution have only minor effects on the location of the M2–M7 dwarfs in the  $(g-r)$  vs.  $(r-i)$  diagram implying that reddening may be isolated in a rather unique way. From  $r$ ,  $M_{r,(r-i)_0}$  and  $E_{g-r}$  we may construct distance vs.  $A_r$  diagrams. This purely photometric method is applied on SDSS DR8 data in the MBM 12 region. We derive individual stellar distances with a precision  $\approx 20$ –26%. For extinctions in the  $r$  – band the estimate is better than 0.2 mag for  $\approx 67\%$  and between 0.3 and 0.4 for the remaining  $\approx 33\%$ . The extinction discontinuities noticed in the distance vs.  $A_r$  diagrams suggest that MBM 12 is at  $\approx 160$  pc and MBM 16 at a somewhat smaller distance  $\approx 100$  pc. The distance for which  $\Delta(A_r)/\sigma(\Delta(A_r)) = 3$ , where  $\Delta(A_r)$  refers to  $\overline{A_{r,on}} - \overline{A_{r,off}}$ , may possibly be used as an indicator for the cloud distance. For MBM 12 and 16 these distance estimates equal 160 and 100 pc, respectively

**Key words:** molecular clouds – interstellar extinction – distances : M dwarf stars.

## 1 INTRODUCTION

MBM 12 is a high latitude molecular cloud and since it has  $A_V$  exceeding 5 mag, Hearty, Neuhäuser, Stelzer et al. (2000), it is classified as a dark cloud. And it contains more than a dozen PMS stars. An active high latitude cloud requires possibly other mechanisms for star formation than dark clouds close to the galactic plane. Estimating parameters essential for initiating star formation, such as the cloud mass and density, depends on the cloud distance. We include MBM 16, a high latitude neighboring translucent cloud, only ten degrees removed from MBM 12, and showing no star formation. For a recent review of high latitude molecular clouds McGehee (2008) may be consulted.

The MBM 12 distance has a long long history and a corresponding, large variation. Shortly after its inclusion in the MBM catalog Hobbs, Blitz, and Magnani (1986) suggested  $\sim 65$  pc as derived from NaI spectroscopy and spectroscopic distances of a small sample of stars. Hobbs et al. (1988) suggest the same distance for MBM 16 about ten degrees away from MBM 12. The estimate for MBM 12 was altered by Hearty, Neuhäuser, Stelzer et al. (2000), after Hipparcos parallaxes became available, to the range from

58 to 90 pc. Again lower and upper estimates were based on the absence/presence of NaI absorption. Luhman (2001) and Andersson et al. (2002) have used more indirect methods and prefer a cloud distance of 275 pc and  $360 \pm 30$  pc, respectively. Both of these papers do, however, detect dust, thought not to be associated to MBM 12, at 65, 140 pc and at  $\sim 80$  pc respectively. An intermediary distance, 325 pc, is proposed by Straižys et al. (2002) from Vilnius photometry of dwarfs and giants brighter than  $V \approx 12$  mag. That work also indicates the possible presence of a small hump,  $A_V \leq 0.4$  mag, of extinction at 140–160 pc.

Accurate and homogenous SDSS *griz* photometry has proven useful for deriving distances and extinction estimates for stars in the M dwarf range within  $\approx 1$  kpc (e.g. Jones, West and Foster 2011). Our own interest in using *griz* photometry for 3-D mapping of the ISM was inspired by the stellar models by Girardi et al. (2004). These models convinced us that the position of the  $(g-r)_0 - (r-i)_0$  locus was influenced very little by variation in  $[M/H]$ , and by ages varying from a few million years to the age of the Milky Way. The latter invariance was perhaps to be expected. Furthermore, and most important, the reddening ratio  $E_{r-i}/E_{g-r}$  has a value, Girardi et al. (2004), that approximates the slope of the main sequence, in the  $(g-r)$  –  $(r-i)$  diagram, for dwarfs earlier than  $\sim M1$ . A consequence is, that red-

\* E-mail: indus@nbi.ku.dk (JK); heplindstroem@yahoo.dk (HL)

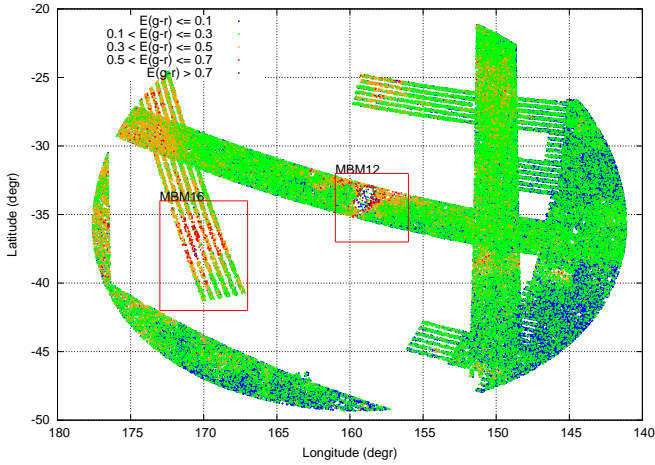


**Figure 1.** MBM 12 *region*. SDSS DR8 M2 - M7 dwarfs with  $\sigma_{gri} < 0.060$  mag and less than  $15^\circ$  from the nominal center of MBM 12. The MBM 12 and MBM 16 *areas* outlined. The resulting color excesses are color coded

dening seems to be the only parameter that shifts observed  $(g-r)$ ,  $(r-i)$  pairs away from the intrinsic locus. Another fact that makes the *gri* photometry so useful for M dwarfs is the good relation,  $\sigma_{M_r} \approx 0.4$  mag, between  $(r-i)_0$  and the absolute magnitude  $M_r$ : a range of  $\approx 2$  mag in  $(r-i)_0$  corresponds to a range of  $\approx 9$  mag in  $M_r$ . This is taken from Table 2 of West et al. (2011) together with the equation for  $M_{r,(r-i)_0}$ , Table 4 of Bochanski, Hawley, Covey et al. (2007) valid for the 0.62 – 2.82 range of  $(r-i)_0$ . The absolute magnitude calibration have required precise distances for a representative sample, Table 4.1, Bochanski (2008).

We apply the photometric parallax and investigate the variation of extinction with distance in a region with a radius  $15^\circ$  centered on the high latitude, dark cloud MBM 12. This region is known to contain several clouds with molecular gas, e.g. the extended translucent cloud MBM 16. The locations of these clouds are interesting because of their various state of activity and their position relative to the confinement of the local cavity.

## 2 M DWARF SAMPLE SELECTION FROM SDSS DR8

To establish a sample of M dwarfs we follow a selection procedure in line with Jones, West and Foster (2011). The candidate sample is drawn from the most recent SDSS data release, DR8, applied for a region, centered on the MBM 12 position  $(l, b) \sim (159.^\circ 4, -34.^\circ 3)$  with a  $15^\circ$  radius, as shown in Fig. 1. The coverage is incomplete but several MBMs are partially scanned. Using the DR8 CasJobs tool we queried for STAR objects with CLEAN photometry for  $g$ ,  $r$ ,  $i$  and  $z$ , respectively, and fulfilling the selection criteria:  $\sigma_{g,r,i} < 0.06$  mag,  $(r-i) > 0.53$  mag and  $(i-z) > 0.3$  mag. The cuts in  $(r-i)$  and  $(i-z)$  contribute to minimize the contamination by (partially) eliminating quasars, giants and M flare stars. Aspects of the sample are shown in Fig. 2. Notice how the reddening of the main sequence stars earlier than  $\sim M1$  does not contaminate the location of reddened M dwarfs.

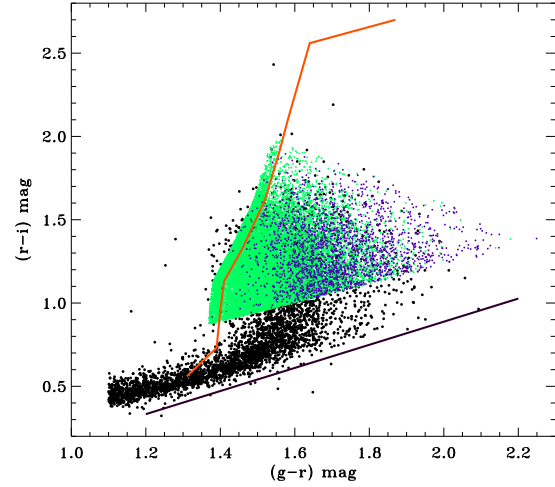


**Figure 2.**  $(r-i)$  vs.  $(g-r)$  diagram. Black points are a selection of stars from the region in Fig. 1. The green symbols are M dwarfs selected in the MBM 12 area. Blue symbols are M dwarfs selected in the MBM 16 area. Notice that the earliest M dwarfs among the MBM 16 stars are shifted to the red of the standard locus which may indicate the presence of some very local dust. The solid jagged line is the standard  $(g-r)_0-(r-i)_0$  locus from West et al. (2011) Table 2 given as the median color of each spectral type  $M0, \dots, M9$ . The slope of the cut off equals the reddening ratio  $E_{r-i}/E_{g-r} = 0.694$ , Girardi et al. (2004), indicated by the straight line

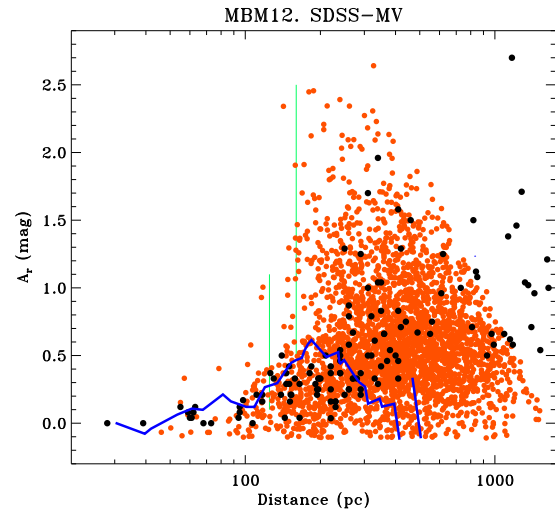


**Figure 3.** Distance vs. extinction diagram for the MBM 12 area. Red symbols are for the MBM 12 area exclusively. The vertical line at 160 pc indicates our suggested MBM 12 location. For comparison the black points are the data, with  $A_V$  converted to  $A_r$ , on which a MBM 12 distance of 325 pc was based, Straižys et al. (2002). The blue curve is  $\overline{A_r}$  from Hipparcos data

## 3 EXTINCTION AND DISTANCE ESTIMATION. UNCERTAINTY

The linchpin for our work is the  $(r-i)$  vs.  $(g-r)$  diagram, which is characterized by showing only minor  $(g-r)_0$  variation for M dwarfs. The  $(r-i)$  vs.  $(g-r)$  reddening vector has

a slope almost identical to the slope of the main sequence earlier than  $\sim M1$ - $M2$  meaning that reddened dwarfs earlier than this limit do not contaminate the location of reddened dwarfs later than  $\sim M2$ . See Fig. 2 where the M dwarf standard locus starts at M0. As judged from the evolutionary models by Girardi et al. (2004) the chemical composition and evolution have minor effects on the location of the M dwarfs in the  $(r-i)_0$  vs.  $(g-r)_0$  diagram. According to Bochanski et al. (2007)  $(g-r)$  colors are likely to depend on metallicity but no clear trends are apparent for  $(r-i)$  and  $(g-r)$ . M dwarf activity in the form of flares mostly effects the blue part of the spectrum, i.e. the  $u$  and the  $g$  bands implying that  $g-r$  is affected but not  $r$ . According to West et al. (2008) a flare will typically change  $g-r$  to values below 0.05 mag. As Fig. 2 shows the  $g-r$  range we consider is far redder than this and  $E_{g-r} > 1.4$  or  $A_r > 4$  is required to shift a flaring star into the color range we use. For the variation in  $M_{r,r-z}$  with magnetic activity and metallicity see, however, the discussion by Bochanski, Hawley, West (2011). A more serious contamination can be caused by unresolved binarity and depends on the components mass ratio. With a mass ratio of one the colors do not change but the observed  $r$  magnitude is decreased by 0.75 mag. The estimated  $M_r$  is not influenced since the  $(r-i)$  and  $(g-r)$  colors are left unchanged. For an individual target, binarity introduces a distance uncertainty  $\approx 35\%$  with a unit mass ratio. The estimated extinction is accordingly not altered but its location is shifted to a larger distance. A recent paper, Clark, Blake and Knapp (2012) has estimated the fraction of close,  $a < 0.4$  AU, M dwarf binaries to 3–4%. Dwarfs later than M6 has a frequency of  $20 \pm 4\%$ , Allen (2007) and the overall binary frequency among M dwarfs is  $42 \pm 20\%$ , Fischer and Marcy (1992).

In Fig. 2 is shown three aspects of the  $(r-i)$  vs.  $(g-r)$  diagram for the MBM 12 region sample. The black points are a selection the region stars. The green symbols are M dwarfs in the MBM 12 area. Blue symbols signify M dwarfs in the MBM 16 area. True color excesses are positive but due to observational errors in  $(r-i)$  and  $(g-r)$  unreddened and little reddened stars are sometimes shifted to the blue of the  $(r-i)_0$  vs.  $(g-r)_0$  locus. In Fig. 2 we have indicated the one sigma confinement based on the maximum error 0.060 mag in  $g, r, i$ . This confinement is corroborated by the scatter around the standard locus of M dwarfs observed at the virtually unreddened North Galactic Pole.

### 3.1 Estimate of the Extinction $A_r$

As the sample of nearby M dwarfs, forming the basis for the standard locus, shows there is a scatter around the standard locus even for virtually unreddened stars. But collapsing the main sequence to a sharp relation has often proven useful. In a previous section we have argued that a shift from the locus may mainly depend on reddening. The intrinsic location of a dwarf is on the locus and is determined by translating the observation position along a reddening vector. The color shifts  $\Delta(g-r)$  and  $\Delta(r-i)$  are accordingly assumed to equal  $E_{g-r}$  and  $E_{r-i}$  respectively.

$\frac{E_{r-i}}{E_{g-r}} = 0.694$  is adopted from Girardi et al. (2004) calculated with  $A_V = 0.5$  mag,  $R = 3.1$ ,  $T_{eff} = 3500$  K,  $\log(g) = 4.5$  and  $[M/H] = 0$ . Not ideal but rather close to the M range.

We have  $A_r = 2.875 \times E_{g-r}$ , also adopted from Girardi et al. op. cit. For  $(r-i)$  the relation is  $A_r = 4.142 \times E_{r-i}$ . The ratio between the two coefficients is 1.441 so other things being equal  $E_{g-r}$  is preferred due to a more favorable error progression.

### 3.2 Estimated Distance

Having estimated  $A_r$  and observed  $r$  only  $M_r$  is missing for the photometric parallax. We rely on the calibration of  $M_r$  in terms of  $(r-i)_0$  which is preferred to  $(g-r)_0$  due to a better error progression. The  $M_r$  calibration of  $(r-i)_0$  for M dwarfs is as mentioned adopted from Bochanski, Hawley, Covey et al. (2007).

The distance estimate is derived from the usual formula:

$$distance = 10^{0.2 \times (r - M_r - A_r + 5)} \quad (1)$$

where all parameters are known together with their uncertainties.

### 3.3 Uncertainties on Extinction and Distance

Each entry in the extraction from SDSS DR8 contains errors on all magnitudes but we have preselected stars with  $\sigma_{gri} < 0.060$  mag. We may estimate the total uncertainty from the combination of observational errors and errors introduced from the calibrations.

If  $s = f(x_i)$  represents either the full set of equations used to estimate  $A_r$  or  $M_r$  the formal error of  $s$  follows from the progression formula:

$$\sigma_s^2 = \sum_i \left( \frac{\partial s}{\partial x_i} \sigma_{x_i} \right)^2 \quad (2)$$

For each star we compute  $\frac{\partial s}{\partial x_i}$  and  $\sigma_{x_i}$  implying that derivatives must be calculated and errors of the independent parameters also must be known. The errors  $\sigma_{(g-r)_0}$  and  $\sigma_{(r-i)_0}$  are derived from piecemeal linear approximations to the intrinsic locus, taking into account errors in slope and intersection, together with the observational errors in  $g, r$  and  $i$ .  $\sigma_{M_r}$  is calculated from the calibration equation (1) considering our individual, estimated errors  $\sigma_{(r-i)_0}$ .

The resulting uncertainties are in the range 20–26% for the distances and for  $A_r$  about 2/3 has  $\sigma_{A_r}$  in the range from 0.04 to 0.20 mag and about 1/3 between 0.30 and 0.40. The reason for this double peaked distribution is the kink in the intrinsic locus noticed in Fig. 2

## 4 RESULTS

SDSS DR8 provides a substantial amount of M dwarf data for the MBM 12 region and the distance and  $A_r$  accuracies are adequate to study the distance - extinction variation.

### 4.1 MBM 12 Distance Estimate

The distance to MBM 12 is particularly interesting because the cloud is a specimen of a rare variety, high latitude, dark cloud ( $A_V > 5$  have been measured) that even shows star formation activity.

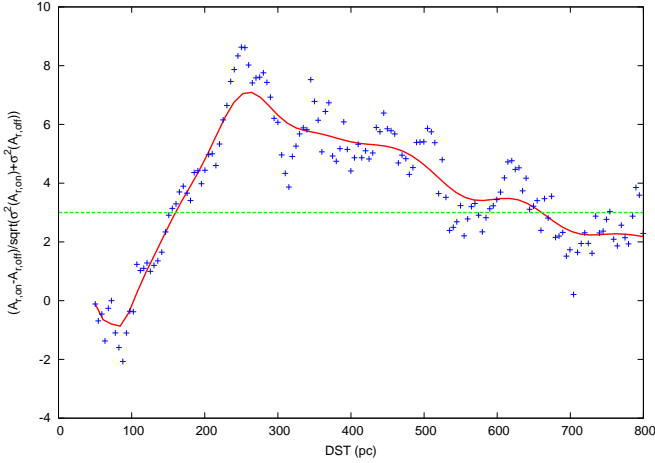


**Figure 4.** The  $\frac{\Delta A_r}{\sigma(\Delta A_r)}$  ratio for the MBM 12 dark cloud. Points are from 30 pc distance bins, stepsize 10 pc. Neighboring points thus not independent. The curve is a Bezier smoothing of the data. The ratio equal 3 at 160 pc which is proposed as the cloud distance

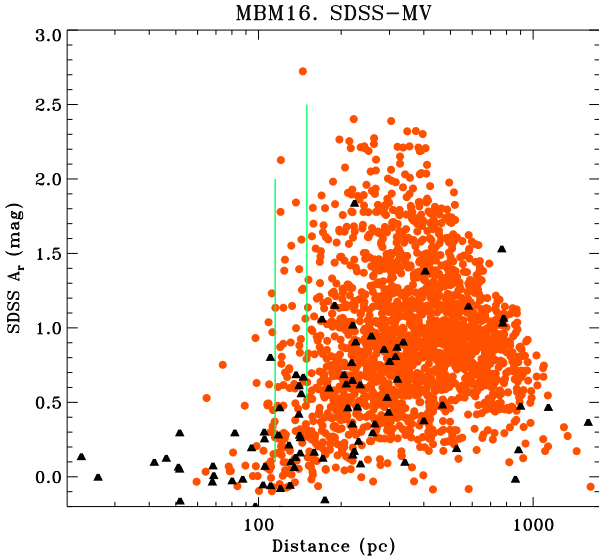


**Figure 5.** Extinction vs. distance for the MBM 16 area. Note that beyond  $\sim 200$  pc most stars have  $A_r > 0.3$  mag. The vertical line indicates that the distance of the first dust is at 102 pc. The MBM 12 distance at 160 pc is also indicated. Black triangles are Hipparcos data for the MBM 16 area with  $A_r$  extinctions. The star HIP 14997 was left out, it has an uncertain  $B - V$  and is listed as a variable, Koen and Eyer (2002)

#### 4.1.1 Distance from appearance of substantial extinction

By substantial extinction we mean an extinction that appears in a discontinuity and is substantially larger than the extinction at smaller distances and that several stars do show such an extinction.

From the  $M_r$  luminosity calibration of  $(r - i)_0$  and the color excess from  $(g - r) - (g - r)_0$  in Fig. 2 we construct a distance vs.  $A_r$  diagram for the MBM 12 area, as shown by the red dots in Fig. 3. We have used a logarithmic distance scale to emphasize the smaller distances.

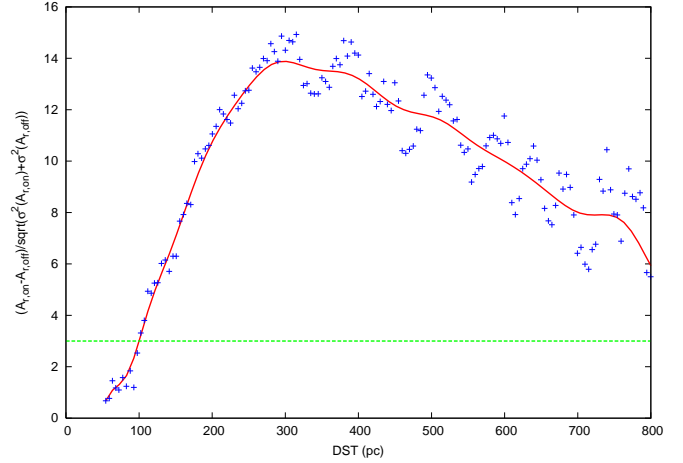


**Figure 6.** The  $\frac{\Delta A_r}{\sigma(\Delta A_r)}$  ratio for the MBM 16 translucent cloud. The diagram proposes a cloud distance of  $\sim 100$  pc significantly shorter than the  $\sim 160$  pc suggested for MBM 12

Apparently there is a rise in  $A_r$  beyond  $\sim 0.5$  mag around 100 pc. We have shown a vertical line at 125 pc. There are some MBM 12 stars with extinction  $\approx 1$  mag at  $\approx 125$  pc but the dominating increase takes place at  $\sim 162$  pc indicated by a vertical line too. Since this distance is somewhat smaller than the presently preferred range discussed in the introduction we have compared to the distance vs. extinction variation derived from the Hipparcos Catalog. We have extracted Hipparcos stars in the MBM 12 area, same  $l$  and  $b$  limits as used for the SDSS extraction. Parallaxes are from the second derivation by van Leeuwen (2007) and extinctions are from  $B, V$  photometry and spectral classification, see e.g. Knude and Høg (1998). The extinction is averaged in 30 pc intervals and is given as the blue solid curve in Fig. 3. The Hipparcos curve is seen to follow the upper envelope of the MBM 12 extinction rather well. Since the Hipparcos sample has a rather bright limiting magnitude, Perryman, Lindegren, Kowalevsky et al. (1995), we can only expect to see smaller extinctions. If we accept the distance of the onset of extinctions beyond, say one magnitude, which is  $\approx 3\sigma_{A_r}$  above 0, as the cloud distance, MBM 12 is at 160 pc.

#### 4.1.2 Alternative distance derivation for MBM 12

The scans in Fig. 1 cover several clouds revealed by their color excesses but also sight lines with less dust. One may expect that for a small distance bin at a given distance the average extinctions in a cloud direction and outside the clouds differ. For distances less than the cloud distance, but in the direction of a cloud, the two averages will be more similar. As Fig. 3 shows there is a substantial scatter of  $A_r$  at almost any distance. A scatter caused by real variation in the presence of dust causing the extinction and the observational errors,  $\sigma_{total}^2 = \sigma_{ISM}^2 + \sigma_{obs}^2$ . If  $\overline{A_{r,on}}$  and  $\overline{A_{r,off}}$  designate the average extinctions on and off a cloud for identical distance bins we propose that  $\Delta(A_r) = \overline{A_{r,on}} - \overline{A_{r,off}}$  will measure the presence of a cloud at a given distance where the difference is sufficiently large. We use  $\sigma^2(\Delta(A_r)) = \sigma_{total,on}^2 + \sigma_{total,off}^2$  as a measure of the significance of  $\Delta(A_r)$  and define the



cloud distance as the distance when  $\Delta(A_r)/\sigma(\Delta(A_r))$  equals three.

We have done this for the MBM 12 area and compared to the region outside the MBM 12 area as shown in Fig. 4. The individual points are not independent: bin size is 30 pc with a steplength of only 10 pc. The horizontal line is at three and intersects the  $\Delta/\sigma$  curve at 160 pc. Which we accept as the distance to MBM 12.

## 4.2 The distance to MBM 16

Another cloud in the MBM 12 region is MBM 16 which is of different type than MBM 12. MBM 16 is translucent whereas MBM 12 is a dark cloud. The two types are distinguished by their optical extinction: a dark cloud has  $A_V > 5$  mag whereas a translucent cloud is less opaque with  $A_V$  in the range from 1 to 5, van Dieshoeck and Black (1988). MBM 16 has been studied by Magnani, Chastain, Kim et al. (2003) in order to understand the origin of turbulence and the correlations between molecular gas and color excesses. For their investigation a distance of 100 pc was assumed, identical to the distance to the wall of Local Bubble as estimated by Cox and Reynolds (1987). In their probing of the local low density cavity Lallement, Welsh, Vergely et al. (2003) suggest the presence of a region with a high density at a distance closer than 100 pc in the direction of MBM 16.

In Fig. 5 is shown SDSS for what is available inside the area shown in Fig. 1. Hipparcos 2 results from the same area is overplotted and two vertical lines at 115 and 160 pc respectively. From the occurrence of the first dust,  $A_r$  ranging from  $\approx 0.5$  to  $\approx 2$  mag, we would suggest  $\sim 115$  pc. Smaller than the MBM 12 distance of 160 pc. The  $A_r$  data from Hipparcos 2 corroborates this to some degree, but only by two stars with  $A_r$  in the range from 0.5 to 1 mag.

The  $\Delta(A_r)/\sigma(\Delta(A_r))=3$  criterion indicates a distance 100 pc for MBM 16 as shown in Fig. 6.

## 5 CONCLUSIONS

We have applied two different methods, which perhaps could be termed qualitative and quantitative, respectively, for estimating the distance to the two high latitude clouds MBM 12 and 16: the distance at which substantial extinction is first measured and the distance where the ratio  $\Delta(A_r)/\sigma(\Delta(A_r))$  equals three. In the case of MBM 12 and 16 the two methods agree. Our suggested distances are 160 for MBM 12 and 100 pc for MBM 16. The former does not agree with the current values from the literature whereas the latter does, almost exactly. That either method works depend on the nice behaviour of the M2–M7 dwarfs in the  $(g-r)$  vs.  $(r-i)$  diagram.

The difference of the MBM 12 and 16 distances has been narrowed from  $\approx 350$ –100 pc to 160–100 pc. The possibility that MBM 12 is outside the confinement of the local bubble and MBM 16 is on or inside still exist. Tempting to suggest that their dark/translucent status is a consequence of their different interstellar environment?

The  $\Delta(A_r)/\sigma(\Delta(A_r)) = 3$  criterion may possibly be expanded to a generalized method for locating nearby molecular clouds where *griz* photometry is available and

maps, 2D and 3D, could be produced with a larger number of stars than used in the spectroscopic study by Jones, West and Foster (2011).

## ACKNOWLEDGMENTS

Our investigation of the Milky Way ISM is financially supported by FNU, grant 09-060601, and Fonden af 29. December 1967.

Funding for the Sloan Digital Sky Survey (SDSS) and SDSS-II has been provided by the Alfred P. Sloan Foundation, and the Participating Institutions.

## REFERENCES

- Allen, P.R., 2007, *ApJ* 668, 492
- Andersson, B.-G., Idzi, R., Uomoto, Alan, Wannier, P. G., Chen, B., Jorgensen, A. M., 2002, *AJ*, 124, 2164
- Bochanski, J.J., 2008, Doctoral Dissertation, University of Washington
- Bochanski, J.J., West, A.A., Hawley, S.L., Covey, K.R. , 2007, *AJ* 133, 531
- Bochanski, J.J., Hawley, S.L., Covey, K.R. et al., 2010, *AJ* 139, 2679
- Bochanski, J.J., Hawley, S.L., West, A.A., 2011, *AJ* 141, 98
- Clark, D.A., Blake, C.H., Knapp, G.R., 2012 *ApJ* 744, 119
- Cox, D.P. and Reynolds, R.J. 1987 *ARA&A* 25, 203
- Fischer, D.A. and Marcy, G.W. 1992 *ApJ* 396, 178
- Girardi, L., Grebel, E.K., Odenkirchen, M., Chiosi, C., 2004, *A&A* 422, 205
- Hearty, T., Neuhäuser, R., Stelzer, B. et al. , 2000, *A&A* 353, 1044
- Hobbs, L.M., Blitz, L., Magnani, L., 1986, *ApJ* 306, 109
- Hobbs, L.M., Penprase, B.E., Welty, D.E., Blitz, L., Magnani, L., 1988, *ApJ* 327, 356
- Jones D.O., West A.A., Foster J.B., 2011, *AJ* 142, 44
- Knude, J. and Høg, E. 1998 *A&A* 338, 897
- Koen, C., Eyer, L. 2002 *MNRAS* 331, 45
- Lallement, R., Welsh, B.Y., Vergely, J.-L., Crifo, F., Sfeir, D., 2003, *A&A* 411, 447
- Luhman K.I., 2001, *ApJ*, 560, 287
- Magnani, L., Chastain, R.J., Kim, H.C., Hartmann, D., Truong, A.T., Thaddeus, P. 2003, *ApJ* 586, 1111
- McGehee, P. M., 2008, Handbook of Star Forming Regions, Volume II, The Southern Sky ASP Monograph Publications, 5, 813
- Perryman, M.A.C., Lindegren, L., Kowalevsky, J. et al., 1995, *A&A* 304, 69
- Straižys V., Černis, A., Kazlauskas and Laugalys, V., 2002, *Baltic Astronomy* 11, 231
- West, A.A., Hawley, S.L., Bochanski, J.J., et al., 2008 *AJ* 135, 785
- West, A.A., Morgan, D.P., Bochanski J.J. et al., 2011, *AJ* 141, 97
- van Dieshoeck, E.F., John, J.B., 1988, *ApJ* 334, 771
- van Leeuwen, F., 2007, *A&A* 474, 653

This paper has been typeset from a  $\text{\LaTeX}$  file prepared by the author.